

Simulation of wake effects between two wind farms.

KS Hansen¹, P-E Réthoré¹, J Palma², BG Hevia³, J Prospathopoulos⁴, A Peña¹, S Ott¹, G Schepers⁵, A Palomares⁶, MP van der Laan¹ and P Volker¹

¹DTU Wind Energy-DK, ²UPorto-PT, ³CENER-ES, ⁴CRES-GR, ⁵ECN-NL and ⁶Ciemat-ES

E-mail: kuhan@dtu.dk

Abstract. SCADA data, recorded on the downstream wind farm, has been used to identify flow cases with visible clustering effects. The inflow condition is derived from a partly undisturbed wind turbine, due to lack of mast measurements. The SCADA data analysis concludes that centre of the deficit for the downstream wind farm with disturbed inflow has a distinct visible maximum deficit zone located only 5-10D downstream from the entrance. This zone, representing 20-30% speed reduction, increases and moves downstream for increasing cluster effect and is not visible outside a flow sector of 20-30°. The eight flow models represented in this benchmark include both RANS models, mesoscale models and engineering models. The flow cases, identified according to the wind speed level and inflow sector, have been simulated and validated with the SCADA results. The model validation concludes that all models more or less are able to predict the location and size of the deficit zone inside the downwind wind farm.

1. Introduction

The EERA-DTOC project (European Energy Research Alliance – Design Tools for Offshore wind farm clusters) is aiming at creating a robust, easy to use and flexible tool to facilitate the optimized design of individual or cluster of offshore wind farms [1, 2].

The wake modeling part of EERA-DTOC has been used to improve the fundamental understanding of wind turbine wakes and modeling. A number of wake cases for large offshore wind farms have been identified. These cases cover a range of conditions, likely to be experienced in offshore wind farms and provide sufficient high-quality input data to form a basis for a systematic evaluation. This includes models from wind farm scale models with straightforward parameterizations for wake behavior through Computational Fluid Dynamics (CFD) models.

This investigation is focusing on benchmarking existing wake modes and in particular their ability to handle the upscaling from wind farm to cluster scale. All benchmark flow cases are defined with reference to existing wind farm measurements, which is used in the validation.

Datasets with potential wake effects within wind farms and between wind farms have been identified and used for the verification. Some of the preliminary flow cases have been reported [3] based on the template from the WakeBench project [4]. The wake models are compared to measurements and possible improvements are identified through three benchmarks:

- 1) The first model validation has been focused on a wind farm with constant spacing (7-10 D), combined with sensitivity analysis of power deficit as function of inflow direction, turbulence or stratification on the Horns Rev offshore wind farm [3, 5].
- 2) The second model validation has been performed on an offshore wind farm, characterized with a small spacing (3.3 – 4.3 D) and two “missing” turbines. Results of this benchmark have been presented [6].
- 3) The third validation has been performed on a large wind farm with variable spaced wind turbines, arranged on 5 distinct arches. The last part of the validation encompass a complete wind farm cluster, consisting of two large offshore wind farms with 90 & 72 wind turbines and separated with more than 30D.

This article will present the different models, the wind farm cluster layout, comparison of the measured and simulated wake deficits and the sector wise park efficiency from the third validation.



2. Models

A range of different models used in the benchmarking and their affiliations are listed in Table 1. The models are divided into three groups: engineering models, WRF mesoscale model and CFD models.

Table 1. Models used in the EERA-DTOC benchmark.

DTOC	Models	Affiliation	Mail
1	SCADA/BA	DTU Wind Energy/K.S.Hansen	kuhan@dtu.dk
2	FUGA/SO	DTU Wind Energy/S. Ott	squot@dtu.dk
3	NOJ/GU	DTU Wind Energy/A. Peña	aldi@dtu.dk
4	NOJ/Peña	DTU Wind Energy/A. Peña	aldi@dtu.dk
5	WRF/UPM	CIEMAT/A.Palomares	ana.palomares@ciemat.es
6	WRF/PV	DTU Wind Energy/P.Volker	pvol@dtu.dk
7	AD/RANS	UPORTO/J.L. Palma	jpalma@fe.up.pt
8	CFDWake	CENER/B.G. Hevia	bgarcia@cener.com
9	CRESflowNS	CRES/ J. Prospathopoulos	jprosp@cres.gr
10	FarmFlow	ECN Wind Energy/J.G Scheepers	scheepers@ecn.nl
11	RANS/fpC	DTU Wind Energy/P.van der Laan	plaa@dtu.dk

A short summary of the models are given, but detailed information have been published previously and will only be referred below.

1. SCADA represent the processed wind farm measurements, which are compared to the simulated wake model results. Wind farm SCADA data are usually not referred as a model result in the literature. However, considering the amount of assumptions and processing methods that have to be applied in order to produce comparable results with a wind farm wake model, a processed SCADA data should in all fairness be treated as a model result. This point is further detailed in the succeeding chapters.

2. FUGA is a linearized flow solver based on the steady-state RANS equations, currently only applicable to flat and homogeneous terrain. In FUGA the flow is assumed to be incompressible and lid-driven at the chosen inversion height. It uses a simple eddy viscosity turbulence closure and the Actuator Disk (AD) approach. The model description and validation results are available in [7].

3. NOJ/Peña is a mass-conserving engineering wake model, which is used to estimate the hub-height wind speed downstream of a wind turbine at a given distance. The estimation is based on the hub-height inflow wind speed, known thrust coefficient, rotor radius, wake decay coefficient [8] in combination with the PARK wind farm flow model [9]. The NOJ results are calculated for a distinct, center line direction of the inflow sectors.

4. NOJ/GU is also based on the NOJ model and the results labeled (GU= Gaussian Uncertainty) are calculated for distinct directions and post-processed according to the methodologies described in [10], as function of the directional variability. The GU method is applicable for each of the listed methods.

5. WRF/PV is the Weather Research and Forecasting (WRF) model [11], combined with an Explicit Wake Parametrization (EWP) developed for mesoscale models. A description is given in [12]. The wind turbine is treated as a drag device, which executes a force in the opposite flow direction. In the parametrization, it is assumed that the grid cell pressure field is in average, uninfluenced by the wind turbine and that a wind turbine will cause only additional turbulence due to the enhanced shear production [13].

6. WRF/UPM, also based on WRF, is used to downscale the outputs from the reanalysis data to the domain. The WRF model is coupled to the UPMPARK model [14], which describes the diffusion of multiple wakes in the atmospheric surface layer parameterized by Monin-Obukhov scaling, in order to model the wind flow inside the wind farm.

7. AD/RANS represents the VENTOS®/2 code, which is built around a segregated finite volume implicit method for the solution of the Reynolds averaged Navier-Stokes (RANS) equations for non-

stratified flows, with a two-equation $k-\epsilon$ turbulence model. This Navier-Stokes solver is specifically geared towards the solution of wind flow problems over complex terrain, with a stable core [15, 16] upon which improvements have been added over the years. Modeling the momentum drag associated with the presence of a wind turbine is done implicitly in VENTOS®/2 [17], using a uniformly loaded AD model.

8. CFDWake 1.0 is an elliptic CFD wind farm model, implemented in the open source OpenFOAM, which allows simulating wake effects inside big wind farms through the actuator disk concept. The model is designed for offshore sites where met mast measurements are representative for the freestream flow of all wind turbine positions in the wind farm. CFDWake is implemented as a module of the CFDWind1.0 wind model, designed for the simulation of wind in the Superficial Boundary Layer [18,19,20]. Only simulation results for westerly inflow has been forwarded.

9. CRESflowNS, [21] is a full 3D Navier–Stokes solver using the Wilcox $k-\omega$ turbulence model [22] for turbulence closure. Simulation of the embedded wind turbines is made through the actuator disk theory where the rotor of each wind turbine is simulated as a disk discretized by a number of control volumes. In order to determine the reference velocity for thrust calculation, a parabolic procedure is applied, [23]. The simulation starts without turbines and activates the first row when a certain convergence criterion is fulfilled for the velocities at the wind turbine positions of that row. This procedure is successively repeated until all wind turbine rows are included. Only simulation results for westerly inflow has been forwarded.

10. FarmFlow wake model was originally based on the UPMwake code as developed by the Universidad Polytechnica de Madrid (UPM) [24]. FarmFlow is a 3-dimensional parabolized RANS code with a $k-\epsilon$ turbulence model [25]. The free stream wind field in Farmflow is modelled by taking into account the effect of atmospheric stability through the Monin-Obukhov length and the rotor is modelled as an actuator disk characterized by the thrust curve. The $k-\epsilon$ turbulence parameter adjustments are used to correct for the actuator disk assumptions, based on local field measurements [26].

11. RANS/ f_P C is based on the flow solver EllipSys3D [27-28], where the RANS equations are employed, together with the $k-\epsilon$ - f_P [29] turbulence model, capable of handling the complex near wake flow through a variable eddy-viscosity coefficient. The wind turbines are represented as ADs using a variable force method suited for interacting ADs [30]. Velocity and power deficits predicted by the $k-\epsilon$ - f_P model combined with the variable AD force method compare well with large eddy simulations and measurements, both for single wind turbine wakes [29] and complete wind farms [30]. Furthermore the effect of the Coriolis force on wind turbine wake and wind farm wake interaction has been included by modeling the entire atmospheric boundary layer (ABL) [31].

3. Cluster layout and measurements

The offshore wind farm cluster modelled in EERA-DTOC is located in the southern part of Denmark, 5-10 km outside the coastline, as shown in Figure 1.

The wind farm cluster consists of two large wind farms separated with a distance of 3 km equal to 30 diameters, as shown in Figure 2.

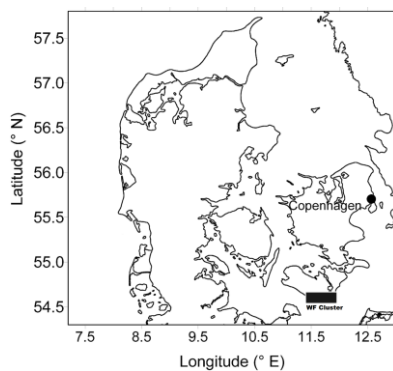


Figure 1. Location of wind farm cluster.

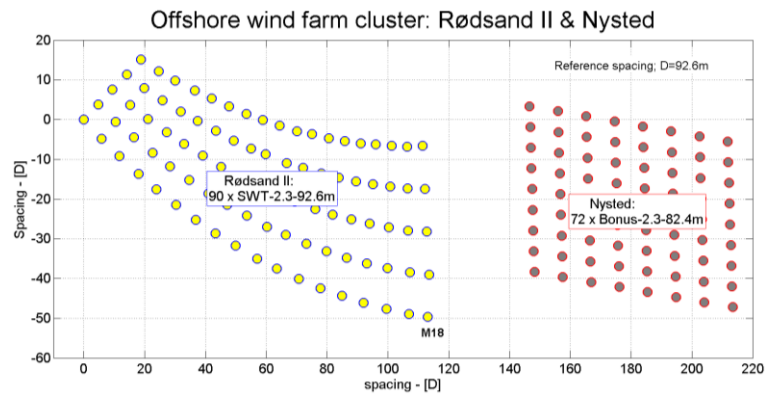


Figure 2. Layout of the wind farm cluster, where the reference spacing is based on SWP-2.3-92.6

3.1 Wind farm layout

Rødsand II offshore wind farm consists of 90 SWP 2.3MW wind turbines with a 92.6 m rotor diameter and a hub height of 68.5 m, partly owned by E.ON. The turbines, which are controlled with a combination of variable speed and pitch, are located on 5 distinct arcs with increased spacing, as shown in Figure 2. The spacing increases from 5D to 10D for changing wind direction. The turbines in Rødsand II wind farm are identical to the turbines presented in the previous EERA-DTOC analysis performed on the Lillgrund offshore wind farm [6]. The wind farm is only equipped with one met mast, located in the south western corner and the wind measurements are very disturbed by the two wind farms for easterly winds.

Nysted offshore wind farm consists of 72 Bonus (later SWP) 2.3MW/82.4m wind turbines, which are active stall controlled, with a hub height of 69 m. This wind farm was commissioned in 2003 and is owned (partly) by DONG Energy A/S. The wind farm includes 4 met masts, located west and east for wind farm. The SCADA dataset from this wind farm has previously been used to intensively wake studies [32]. The internal spacing along the two main directions is $180^\circ/5.7D$ and $97^\circ/10.3D$. Nysted wind farm has been in operation for more than 10 years and obtained an average of 3300 full load hours annually.

3.2 Data sharing and qualification

The SCADA data from Rødsand II includes two periods without time stamp, representing westerly and easterly inflow to the wind farm, for a wind speed range 5-11 m/s. Easterly inflow represent an inflow sector of $70 - 110^\circ$, as shown in Figure 3. The wind farm data is recorded with the (supervisory control and data acquisition) SCADA system as 10-minute statistics for each individual wind turbine in the wind farm. The SCADA signals are: electric power, pitch angle, rotor speed, yaw position and nacelle wind speed.

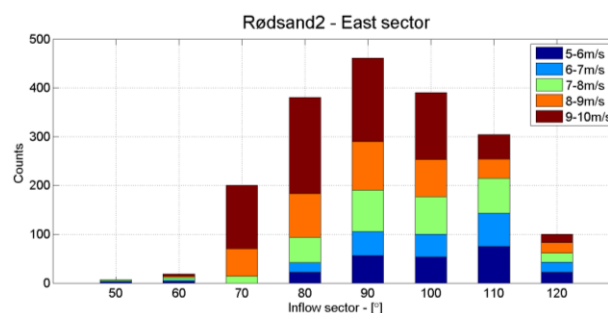


Figure 3. Rødsand II, qualified dataset for easterly inflow.

The SCADA data has been quality-controlled according to the guidelines given in [33, 34]. While the qualification only disqualified 3% of the data and it was decided not to apply further constraints. Due to a lack of measured inflow conditions, it has been necessary to derive the inflow conditions directly from the wind turbines:

- The inflow wind speed at hub height is derived from the measured electrical power combined with the official power curve.
- The inflow direction at hub height is derived from the wind turbine yaw position.

The model comparison is based on wind speed values derived from power values with reference to the official power curve. Unfortunately it has not been possible to verify any of the wind turbine power curves against the official power curve.

The SCADA data from Nysted wind farm includes 2½ years of operation, which has been used in previous flow deficit analysis [34]. The dataset consists of wind farm SCADA data synchronized with meteorological measurements.

Unfortunately there is no synchronized SCADA data representing the whole wind farm cluster. The model validation will focus on the periods where Rødsand II wind farm is online, assuming the Nysted offshore wind farm is online and operating with 100% availability. The Danish wind turbine production register hosted by the Danish Energy Agency reports that the energy production for the Nysted wind farm throughout the period 2011-2014 has been reliable and large.

3.3 Ambient flow conditions

The wind conditions have been measured before the installation of the Rødsand II wind farm and displays a sector wise turbulence intensity (TI) of 7% at hub height for easterly wind at 8 ± 0.5 m/s for the wind direction sector [75-105°].

The average speed recovery behind the Nysted wind farm for easterly inflow has been extracted as function of the inflow angle, and the estimated wind speed reduction is 15% for the inflow sector [80-105°] at wind speed of 8 m/s.

3.4 SCADA data analysis

The normalized speed deficit¹ inside the wind farm is determined with reference to the wind speed at the reference wind turbine M18, which is located in the south eastern corner of Rødsand II wind farm, Figure 2. Unfortunately this wind turbine is operating partly in the wake of Nysted wind farm, as all other Rødsand turbines for easterly wind. The inflow wind speed is derived from the power level, corresponding to 8 ± 0.5 m/s and the inflow wind direction is equal to the wind turbine yaw position.

The normalized speed deficit distribution for the “variable” spaced turbines in the Rødsand II wind farm is difficult to visualize – compared to previous analysis of wind farms with regular layout and fixed spacing. The normalized speed deficit values are therefore illustrated as colored contour plot, as shown in Figure 4. The normalized wind speed deficit distribution for Nysted wind farm is calculated for the wind speed interval 8 ± 0.5 m/s with reference to the measured wind speed at hub height on a mast located 2 km east of the wind farm, for 10 degree sectors. The Rødsand II wind farm reference turbine (=M18) is partly disturbed for $WD=77-97^\circ$ by the Nysted wake. The figures 4b, 4c and 4e demonstrates how the distinct Rødsand II speed deficit zone develops at 87° , increases in size and moves downstream for increasing inflow angle until 107° when the Nysted wake only covers a tiny part of the Rødsand II wind farm.

The integrated effect of the speed deficit distribution is expressed as the sector wise park efficiency, calculated with reference to the top-3 producing wind turbines, using a moving window averaging technique, for a window size of 4° . Figure 5 shows a decreasing park efficiency when the Nysted wake partly covers Rødsand II wind farm. The decrease is a combined wake effect and cluster effect. This effect seems to reach a minimum at 107° , when the Nysted wake has passed the Rødsand II wind farm.

¹ The normalized speed deficit is equal to (1-speed ratio).

Due to the asymmetric layout of the Rødsand II wind farm it is not possible directly to conclude on the park efficiency obtained for western and eastern inflow sector.

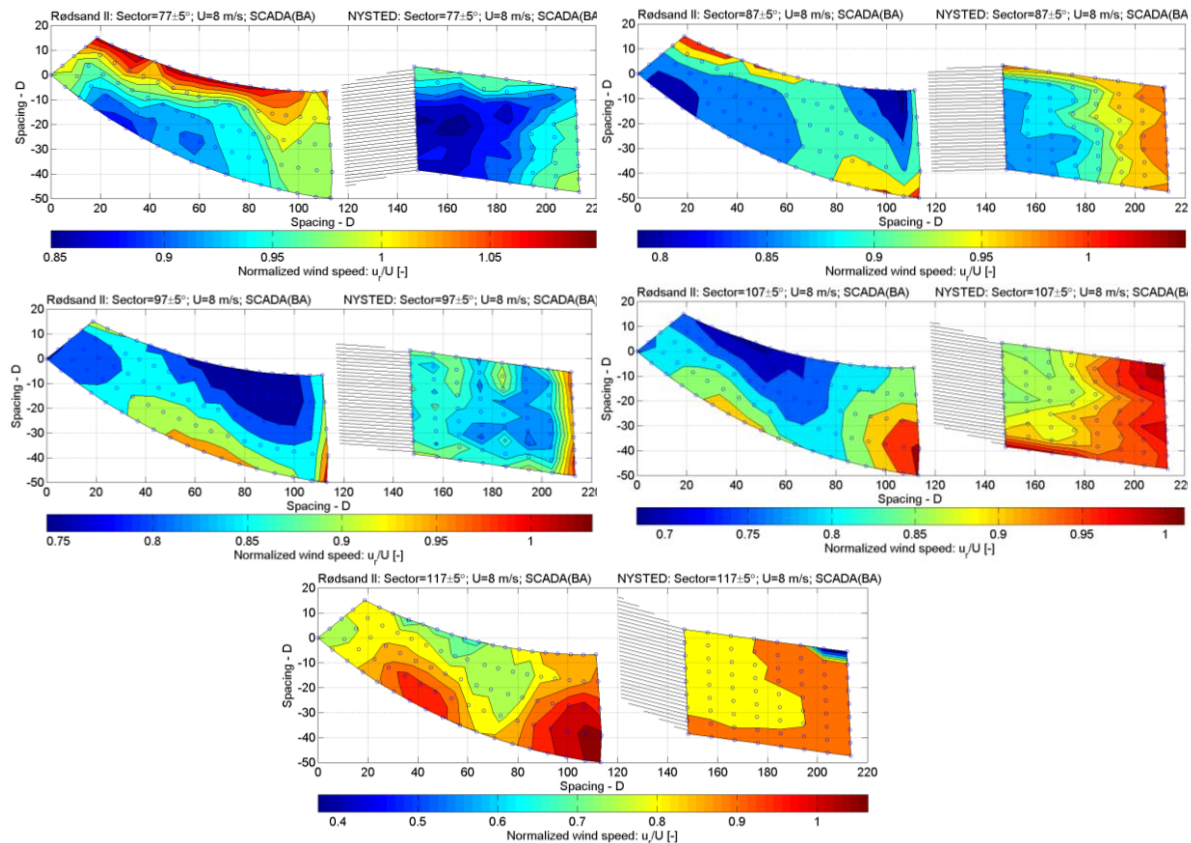


Figure 4. Measured normalized speed deficit distribution on Rødsand II & Nysted wind farm for WD=77, 87, 97, 107, 117 ±5° and U=8 ±0.5 m/s sectors respectively.

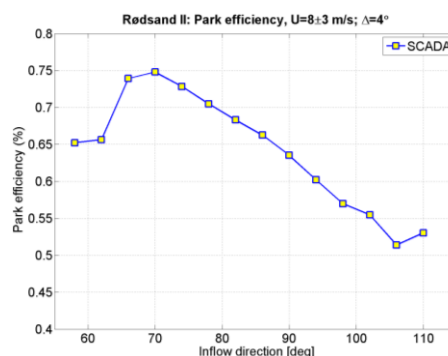


Figure 5. Measured park efficiency for the Rødsand II wind farm.

The SCADA data analysis includes a high uncertainty related to operational wind turbine parameters, which can be summarized as:

- Disturbed inflow to the reference wind turbine, M18;
- Lack of power curve validation and signal calibration;
- Transformation from electric power to wind speed without taking pitch angle and rotor speed into account;
- Wind turbine yaw position depends on the yaw controller, time constants and yaw threshold values;

- The spatial variability of both wind speed and wind direction over very large distance are difficult to take into account.

4. Flow cases

In the easterly wind direction, both wind farms need to be modelled to predict the cluster effect. While there is a limited amount of information available on Rødsand II wind farm and nothing about the operational status of Nysted wind farm, the modellers should assume that all 162 turbines were operating under neutral atmospheric conditions.

The wind farm and cluster wake models are simulated for the inflow conditions applied to the Nysted wind farm, summarized as:

- Inflow wind speeds at hub height is $8 \pm 0.5^\circ$ m/s;
 - Turbulence intensity at hub height is 7%;
 - 5 different inflow sectors, represented with: $[87 \pm 5^\circ, 97 \pm 5^\circ, 107 \pm 5^\circ, 77 \pm 5^\circ, 117 \pm 5^\circ]$ degrees;
- The modellers were asked to model the five distinct inflow directions or the sectors. All modellers should provide the simulated power values for each of the 162 wind turbines for the 5 distinct flow sectors.

5. Results

The model results were divided into two parts; 4 partners submitted results covering the whole wind farm cluster while the remaining 4 modellers submitted results covering only the Rødsand II wind farm - but still taking the influence into account the wake from Nysted wind farm. The model contributions are listed in Table 2.

Table 2. Wind farm cluster simulation matrix

WD=	Rødsand II wind farm					Nysted wind farm				
	77°	87°	97°	107°	117°	77°	87°	97°	107°	117°
SCADA(BA)	x	x	x	x	x	x	x	x	x	x
AD/RANS	x	x	x	x	x	x	x	x	x	x
FarmFlow	x	x	x	x	x	x	x	x	x	x
NOJ/Peña	x	x	x	x	x					
NOJ(GU)	x	x	x	x	x					
FUGA/SO	x	x	x	x	x					
Mesoscale	x	x	x	x	x					
RANS/f_PC	x	x	x	x	x	x	x	x	x	x
WRF/UPM	x	x	x	x					x	

5.1. Discussion

The whole wind farm was modelled as a single grid-cell in the Mesoscale model and the resulting power/wind speed is represented with one single value.

Sector WD=77° demonstrates that the model agrees well, but predicts larger speed reduction compared to the SCADA results with NMAE² values equal to 0.1 ± 0.02 for all models.

The discussion below refers to the presented results compared to SCADA results, shown in Figure 4.

Sector WD=87° on Figure 6, demonstrates that most of the models predict the triangular speed reduction zone in the NE part initiated by Nysted wind farm wake quite well. The NMAE values are equal to 0.04 ± 0.02 .

Sector WD=97° on Figure 7, represents the aligned flow in the Nysted wind farm and demonstrates how the triangular speed reduction zone moves [downstream] towards W for increasing inflow direction

² NMAE is the Normalized Mean Averaged Error from WakeBench [4] and has been calculated with reference to the SCADA values.

for most of the simulated distributions. All the models predicts the deficit well with comparable NMAE values equal to 0.06 ± 0.02 .

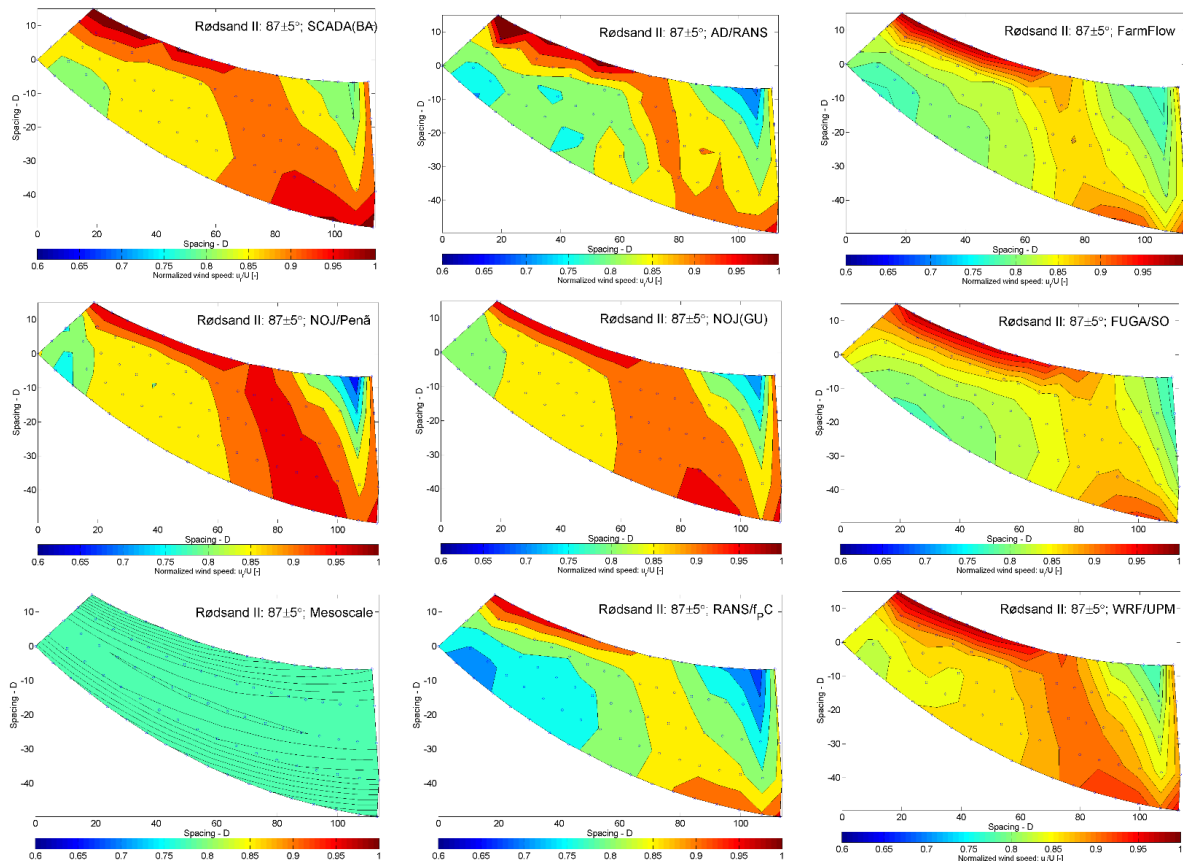


Figure 6. Measured and simulated wake deficit for the Rødsand II wind farm for the inflow sector: $87 \pm 5^\circ$ and $U = 8 \pm 0.5$ m/s.

Sector $WD = 107^\circ$ (plot is not included); despite that most of the Nysted wake influence has vanished, some models still predict a distinct N-S deficit area around $90D$ with a visible speed reduction. All models predict the increased speed around the SE wind farm “corner”, with undisturbed inflow.

Sector $WD = 117^\circ$ (plot is not included), some of the models predicts a large, distinct deficit area, $30D$ from the inlet. All models predict the increased speed around the SE wind farm “corner” with undisturbed inflow. The NMAE values equal to 0.1 ± 0.02 demonstrates a limited scatter compared to the previous sector results.

Figure 8 shows the complete, simulated cluster effect for 2 inflow sectors equal to 87° & 97° . The three models seems to predict very well both the undisturbed area and the location and size of the peak deficit zone.

The park efficiency has been calculated for each of the five flow cases ($U = 8 \pm 0.5$ mm/s) and compared to the measured ($U = 5-11$ m/s) park efficiency in Figure 9. The modelled park efficiency levels varies quite much but all models predicts the minimum efficiency to be located in the sector $[97-107^\circ]$.

5.2. Summary

Previous SCADA analysis concludes that centre of the deficit for a wind farm with variable spacing and undisturbed inflow is located $80-90$ diameters downstream from the inflow turbines. Furthermore, the location of the deficit zone is not very sensitive to the inflow direction and the maximum deficit inside the zone is $20 - 25\%$. The present analysis of disturbed inflow situations concludes that the maximum deficit zone is distinct and located only $5-10D$ downstream from the wind farm entrance. The size of the

deficit zone increases and moves downstream for increasing inflow direction e.g. where the wind farm operates in partly wake conditions.

The eight models in the benchmark includes both RANS models, mesoscale models and engineering models. The flow cases, identified with wind speed and inflow sector, have been simulated and compared with the SCADA results. The validation confirms that a distinct triangular deficit zone appears 5-10D into the wind farm, when the upstream wind farm wake encompass the downwind wind farm. The deficit zone, representing 20-30% speed reduction, increases and moves downstream for increasing inflow direction (partial cluster effect), and the external wake effect disappears outside a flow sector of $\pm 15^\circ$.

The benchmark demonstrates that the models are able to predict cluster performance, but it is difficult to draw a conclusion about which models are in error because of the very large uncertainty of the measurements for this test case. Most models use different physical assumptions to model the wake effect. These differences in assumption have an influence on the prediction accuracy that becomes greater as the wind farms become larger. When there are two wind farms in the wake of one another this effect is even more pronounced.

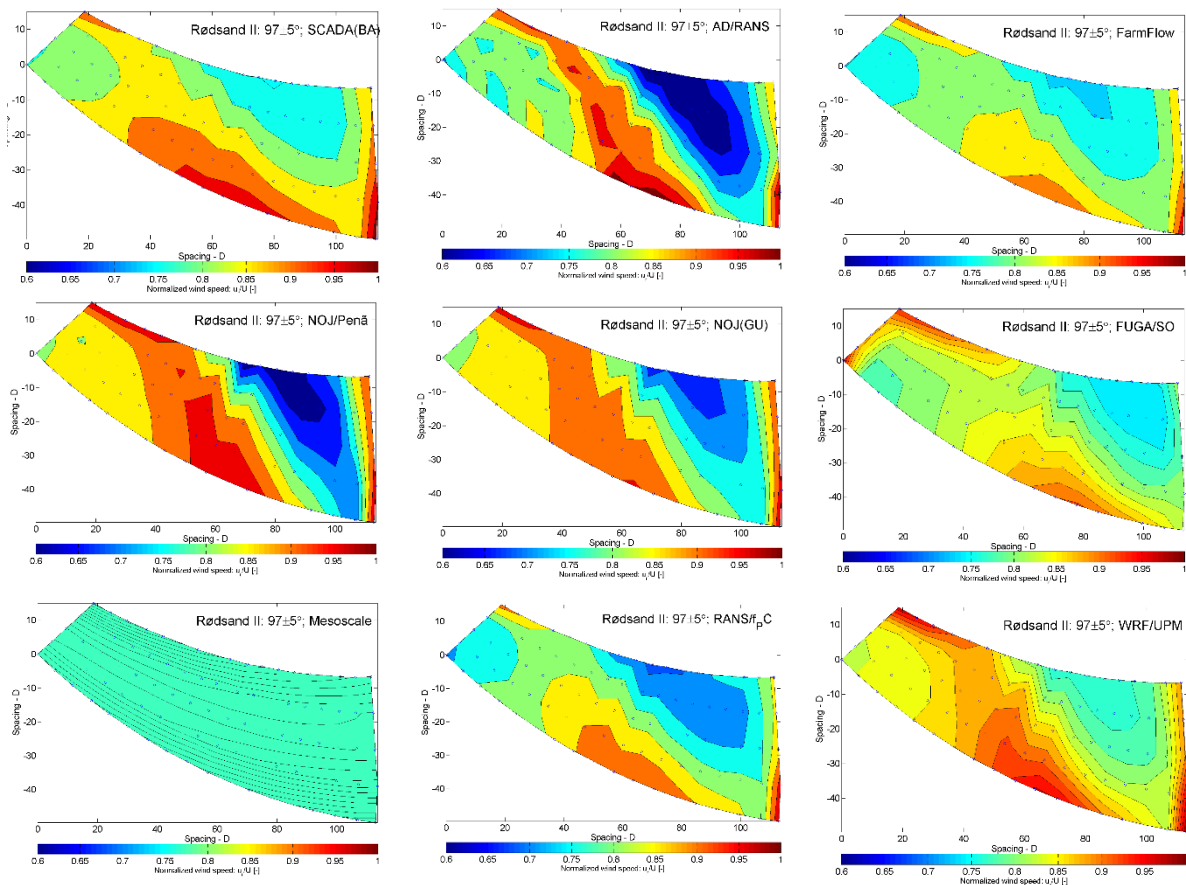


Figure 7. Measured and simulated wake deficit for the Rødsand II wind farm for the inflow sector: $97 \pm 5^\circ$ and $U=8 \pm 0.5$ m/s.

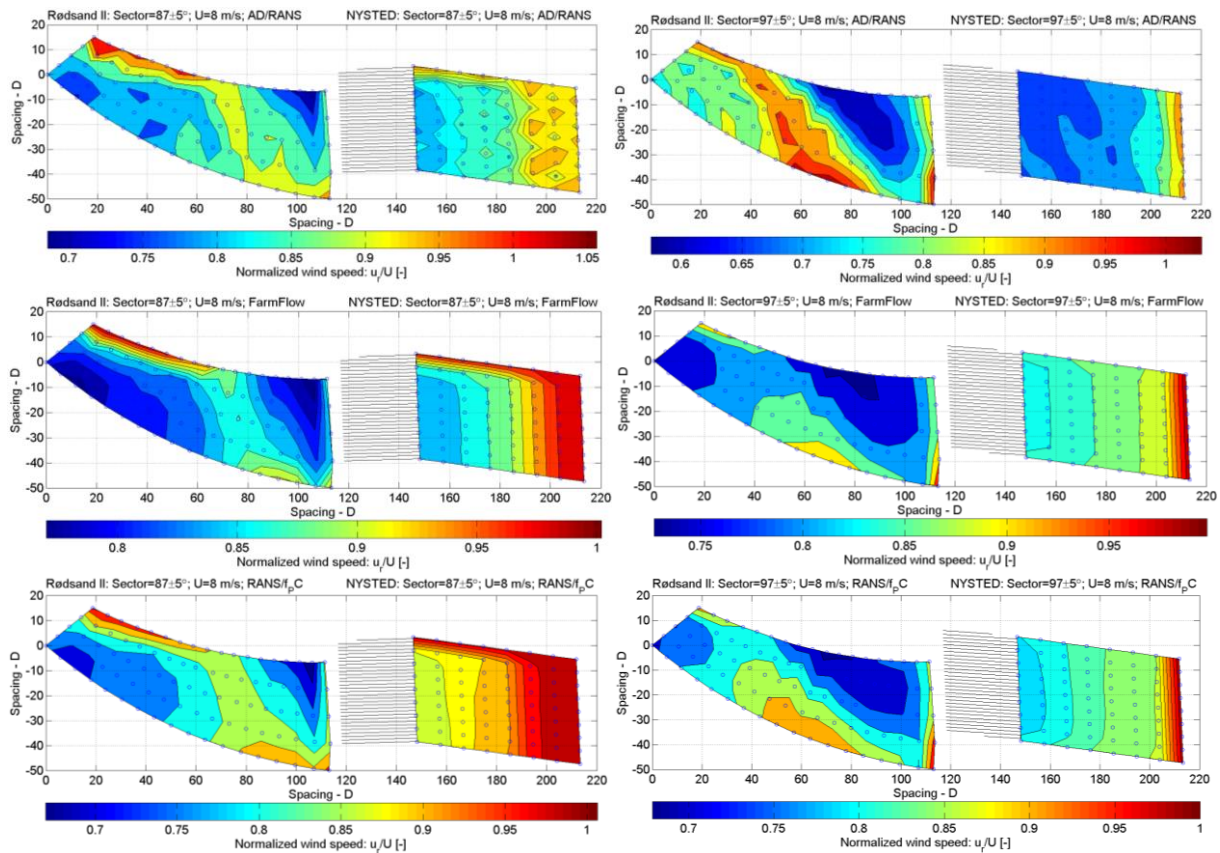


Figure 8. Cluster effect WD=87 & 97±5° inflow sectors.

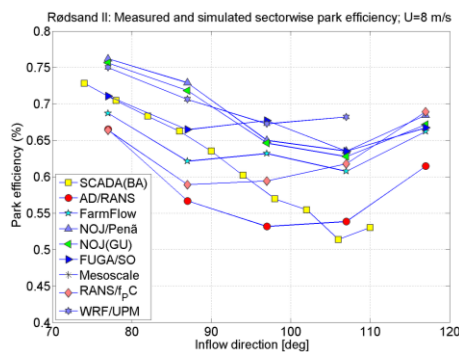


Figure 9. Measured and simulated park efficiency.

6. Conclusion

This is the first investigation that included two wind farms, and the main apparent conclusion is that the models give a significantly large spread, which indicates that there is a need for investigating further these types of flow cases to obtain more robust predictions. The current data we obtained from the wind farm owners are not of sufficient quality in order to draw more meaningful conclusion.

Another way of looking at these comparisons is that the spread of the models illustrate our current predictive capability as the wind energy community. It does encompass the results, which is a good thing, but we should strive at reducing this spread in order to reduce the risks in designing offshore wind farms close to each-other.

7. Acknowledgments

This work was supported by the EU EERA-DTOC project nr. FP7-ENERGY-2011/n 282797. We acknowledge E•ON for having access to the SCADA data from the Rødsand II offshore wind farm and we acknowledge DONG Energy A/S for having access to the SCADA data from Nysted offshore wind farm.

8. References

- [1] <http://EERA-DTOC.EU> project homepage
- [2] Schepers G, et.al. *EERA-DTOC: Design tools for off-shore wind farm clusters including new results on wake bench*; Presented at: European Wind Energy Conference & Exhibition 2013, 2013, Vienna
- [3] Réthoré P-E, et.al. *Benchmarking of wind farm scale wake models in the EERA - DTOC project*, Presented at: International Conference on aerodynamics of Offshore Wind Energy Systems and wakes (ICOWES 2013), 2013, Lyngby
- [4] Moriaty P, et.al. *IEA-Task 31 WAKEBENCH: Towards a protocol for wind farm flow model evaluation. Part 2: Wind farm wake models*, IOP online (DOI: <http://dx.doi.org/10.1088/1742-6596/524/1/012185>), vol: 524, issue: 1, 2014
- [5] Hansen KS, et.al. *The impact of turbulence intensity and atmospheric stability on power deficits due to wind turbine wakes at Horns Rev wind farm*; Wind Energy (ISSN: 1095-4244) DOI: <http://dx.doi.org/10.1002/we.512>, vol: 15, issue: 1, pages: 183-196, 2012
- [6] Hansen KS, et.al. *Benchmarking of Lillgrund offshore wind farm scale wake models*. Presented at: EERA DeepWind 2014 - 11th Deep Sea Offshore Wind R&D Conference, 2014, Trondheim
- [7] Ott S, Berg J, Nielsen M *Linearised CFD Models for Wakes*. Technical Univ. of Denmark, Risoe National Lab. for Sustainable Energy. Wind Energy Div. Risoe-R-1772(EN) ISBN 978-87-550-3892-9. Available online.
- [8] Jensen NO *A note on wind generator interaction*. Technical Report Risoe-M-2411(EN), Risø National Laboratory, Roskilde 1983.
- [9] Peña A, Réthoré PE, Rathmann O *Modeling large offshore wind farms under different atmospheric stability regimes with the park wake model*. Renew. Energ. 2014; 70:164–171.
- [10] Gaumond M et.al. *Evaluation of the wind direction uncertainty and its impact on wake modelling at the Horns Rev offshore wind farm*. Wind Energy 2014; 17:1169–1178.
- [11] Skamarock WC et.al. *A description of the advanced research WRF version 3*. Technical Report TN-475+STR, NCAR, 2008.
- [12] Volker PJ et.al. *The Explicit Wake Parameterization: Development, implementation in the WRF model and evaluation against mast measurements*. Submitted to Geoscientific Model Development.
- [13] Ainsley JF *Calculating the flow field in the wake of wind turbines*. J Wind Eng Ind Aerodyn, 27:213-224, 1988.
- [14] Crespo A, et.al. *UPMPARK: a parabolic 3D code to model wind farms*. Proc. EWEC 1994, European Wind Energy Conference, Thessaloniki, p 454-459.
- [15] Castro F et.al. *Simulation of the Askervein Flow. Part 1: Reynolds Averaged Navier–Stokes Equations (k–ε Turbulence Model)*, Boundary-Layer Meteorology, 2003, 107, 501-530.
- [16] Palma J et.al. *Linear and nonlinear models in wind resource assessment and wind turbine micrositing in complex terrain*, Journal of Wind Engineering and Industrial Aerodynamics, 2008, 96, 2308 – 2326.
- [17] Gomes VMMGC et.al. *Improving actuator disk wake model*, Journal of Physics, Conference Series, 2014, 524, 012170.

- [18] Politis E et.al. *CFD modeling issues of wind turbine wakes under stable atmospheric conditions*, Proceedings of the European Wind Energy Conference, March 2009, Marseille (France).
- [19] Cabezón D et.al. *CFD modelling of the interaction between the Surface Boundary Layer and rotor wake. Comparison of results obtained with different turbulence models and mesh strategies*, Proceedings of the European Wind Energy Conference, March 2009, Marseille (France)
- [20] Cabezón D et.al. *Analysis and validation of CFD wind farm models in complex terrain. Effects induced by topography and wind turbines*, EWEC 2010 scientific proceedings, Warsaw, Poland, April 2010
- [21] Chaviaropoulos PK, Douvikas, DI *Mean-flow-field Simulations over Complex Terrain using a 3D Reynolds-averaged Navier–Stokes Solver*, Proceedings of ECCOMAS '98, Vol. I, part II. Papailiou KD, Tsahalis D, Périaux J, Hirsch C, Pandolf M (eds.). Wiley: West Sussex, England, pp. 842-848.
- [22] Wilcox DC *Turbulence Modelling for CFD*, DCW Industries Inc., La Canada, California, 1993, ISBN 0-9636051-0-0.
- [23] Prospathopoulos JM, Chaviaropoulos PK *Numerical simulation of offshore wind farm clusters*, European Wind Energy Association, Conference proceedings 2013.
- [24] Crespo A et. Al *Numerical Analysis of wind turbine wakes*, Proceedings of Delphi Workshop on "Wind turbine applications, 1985
- [25] Rodi W *Turbulent buoyant jets and plumes* Pergamon Press, 1982
- [26] Schepers JG *Engineering models in Wind Turbine Aerodynamics*, TUDelft, November 2012 ISBN 9789461915078"
- [27] Sørensen NN *General purpose flow solver applied to flow over hills*, 1994 Ph.D. thesis Risø National Laboratory Roskilde, Denmark
- [28] Michelsen JA *Basis3d - a platform for development of multiblock PDE solvers*. 1992 Tech. Rep. AFM 92-05 Technical University of Denmark, Lyngby, Denmark
- [29] Van der Laan MP et.al. *An improved k- ϵ model applied to a wind turbine wake in atmospheric turbulence* 2014 Wind Energy Published online: DOI: 10.1002/we.1736
- [30] Van der Laan MP et.al. *The k- ϵ -fP model applied to wind farms* 2014 Wind Energy Published online: DOI: 10.1002/we.1816
- [31] Van der Laan MP et.al. *Predicting wind farm wake interaction with RANS: an investigation of the Coriolis force*, 2015 Submitted to Wake Conference 2015 in Visby, Sweden
- [32] Barthelmie RJ, Jensen LE *Evaluation of wind farm efficiency and wind turbine wakes at the Nysted offshore wind farm* 2010 Wind Energy Published online: DOI: 10.1002/we.408
- [33] Barthelmie et.al. *Flow and wakes in large wind farms: Final report for UpWind WP8; Appendix 7: Guideline to wind farm wake analysis*, Report Risø-R-1765, January 2011
- [34] Réthoré et al. *Systematic wind farm measurement data reinforcement tool for wake model calibration*, EOW Conference 2009, 14 – 16 September 2009 Stockholm